

## PARAMETER SELECTION RULES FOR ELEMENTS OF ENERGY-ABSORBING STRUCTURES

S. Ochelski, T. Niezgoda

**Military Academy of Technology**  
**Department of Mechanics and Applied Computer Science**  
2 Kaliskiego Street, 00-908 Warsaw, Poland

The paper presents the results of an experimental program and gives suggestions on the design of an energy-absorbing structure with respect to the kinetic energy of impact. The presented results account for the influence of the following factors on the energy-absorbing capability: matrix and reinforcement type, structure, shape and thickness of elements.

**Key words:** polymer composites, absorption energy, experimental testing.

### 1. INTRODUCTION

On the basis of the literature review and the results of our own tests on energy absorbing structures it can be stated that, because of high strength-to-mass ratio, the polymer composites have a wide application in construction of energy-absorbing structures of vehicles and aircrafts. The magnitude of the absorbed

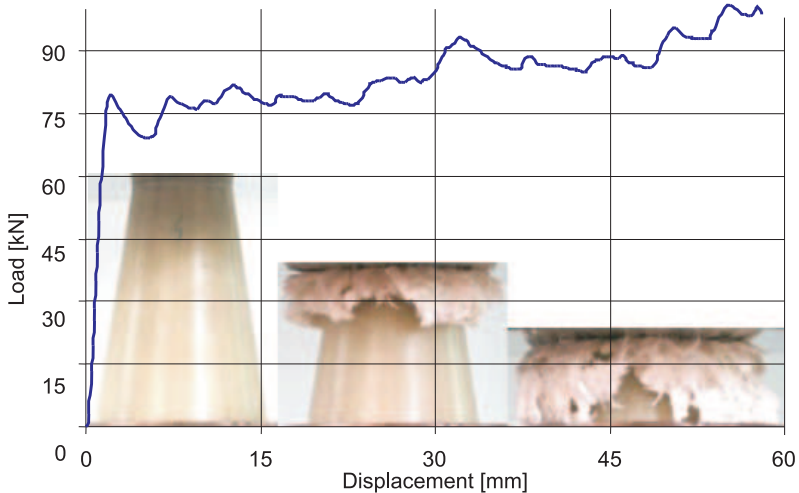


FIG. 1.  $P - \Delta l$  dependence for a truncated cone-shaped specimen made of the epoxy composite reinforced with a glass mat.

energy depends both on the composite type and its components, from which the composite or the sandwich-type structure is made. The energy-absorbing structures, in particular those made of composites, with elements which can acquire various shapes, can be designed to reach the desired value of the absorbed energy, and the mechanism of progressive failure during crash will ensure obtaining of a high absorption energy.

In the paper, an extensive experimental program was carried out on the influence of the type and structure of composites, geometry and shape of an energy-absorbing element. Exemplary relations obtained from the tests were presented in Figs. 1 and 2, from which the progressive failure work has been determined.

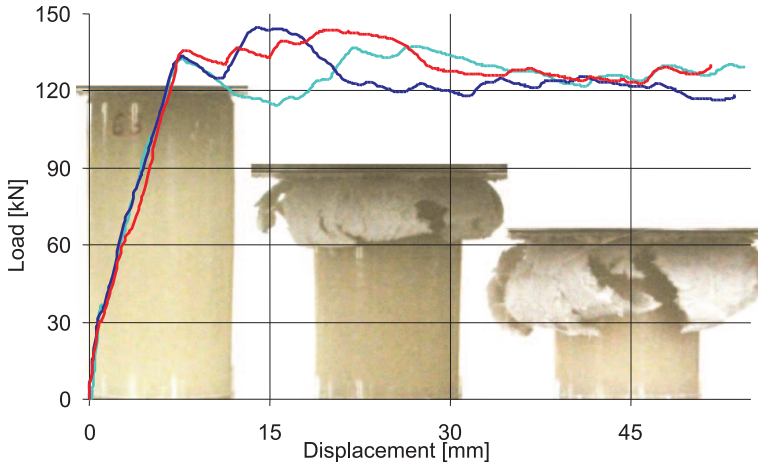


FIG. 2. Crush failure force dependence on displacement for 3 specimens made of the epoxy composite reinforced with a glass mat.

## 2. SELECTION OF THE ENERGY-ABSORBING STRUCTURE PARAMETERS DEPENDING ON THE CRASH ENERGY VALUE

It follows from the work – kinetic energy theorem that:

$$(2.1) \quad -\Delta E = L.$$

The negative increase in the kinetic energy  $\Delta E$  resulting from the crash is equivalent to the work of the crush force  $L$  (absorbed energy)

$$(2.2) \quad -\Delta E = \frac{m \cdot V_k^2}{2} - \frac{mV_0^2}{2},$$

where  $m$  is the object's mass,  $V_0$  – initial velocity,  $V_k$  – final velocity.

Assuming the data obtained from an experimental test of a helicopter crash of a 767 kg mass and the impact velocity equal to 8 m/s, we have

$$(2.3) \quad \Delta E = \frac{767 \cdot 8^2}{2} = 24.544 \text{ kJ},$$

which is equal to the absorbed energy (AE). Knowing the mass of the equipment and its impact velocity, one can calculate the energy value which the absorbing energy structure has to absorb during its failure. Assuming displacement  $\Delta l = 0.1$  m, simple calculations show that the mean crushing force  $P$  is:

$$(2.4) \quad P = \frac{\Delta E}{\Delta l} = 240 \text{ kN}.$$

Assuming that the energy-absorbing structure is of a sandwich type, one can use for its core elements in the shape of tubes, truncated cones, spheres and waved shells. The results of investigation for all these cases in the form of AE will be presented further in the paper.

### 3. COST (PRICE) OF MATERIALS FOR THE ENERGY-ABSORBING STRUCTURES

While selecting materials for energy-absorbing structures, the data included in Table 1 can be useful. To build the energy-absorbing structures of aircrafts, because of the required lightness, mainly various kinds of polymer composites with different types of reinforcement are used. The structure lightness is also important in the automobile industry, because a light car can reach higher accelerations at the same power of the engine. The polymer composites not only have the highest ratio of strength and stiffness to their density, but also the highest specific absorbed energy (SAE), in comparison to metals and their alloys.

The prices of one kilogram of materials given in Table 1 were taken from current price lists (for the year 2006), whereas the SAE values for metals were taken from our own investigations and from literature.

The results presented in Table 1 demonstrate that from among all polymer composites, the epoxy one reinforced with a glass mat reveals the most advantageous ratio of the SAE to the price, whereas it is the carbon steel which, because of its lowest price, proved to have the highest ratio from all the analysed composites and metals. The mean SEA values presented in Table 1 are obtained for various geometries of the absorbing energy structures for the given composite type.

**Table 1. Comparison of SAE with the price of one kilogram for composites and metals.**

Material	Price [USD/kg]	SAE [kJ]	SAE/Price
carbon/epoxy – composite reinforced with roving	60–135	82.3	1.37–0.61
carbon/epoxy – composite reinforced with fabrics	52–120	88.9	1.71–0.74
glass/epoxy – composite reinforced with roving	5.3–10.5	45.1	8.5–4.29
glass/epoxy – composite reinforced with fabrics	4.2–6.5	76.2	18.14–11.72
glass/epoxy – composite reinforced with a mat	2.4–3.2	67.9	28.2–21.21
carbon/PEEK	230–260	128.0	0.55–0.49
aramid/epoxy	60–120	60.1	1.0–0.5
glass/vinylester – composite reinforced with roving	5.1–9.8	50.9	9.98–5.1
glass/vinylester – composite reinforced with fabrics	4.0–5.9	86.1	21.5–14.5
vinylester composite reinforced with carbon roving	58.2–132.1	92.9	1.6–0.79
vinylester composite reinforced with carbon fabrics	53.8–116.7	99.1	1.8–0.85
aluminium alloy	1.4–1.7	18.1	12.9–10.6
carbon steel	0.4–0.9	27.8	69.5–30.8
stainless steel	2.7–3.2	26.8	9.9–8.4

#### 4. INFLUENCE OF MATRIX TYPE (RESIN) AND REINFORCEMENTS (FIBRES) OF POLYMER COMPOSITES

In our investigation we used the matrices and fibres most commonly used in the energy-absorbing structures of aircrafts and automobiles. The following composites were subjected to tests: epoxy, vinylester and polyetherketone ones with carbon, glass and aramid reinforcements of various forms (continuous fibres, fabrics and mat). The results of investigation of the composite matrix influence on the SAE value are presented in Table 1.

On the grounds of the test results presented in Table 2 we can conclude that the highest value of the SAE is revealed by the composites with a polyetherketone matrix (PEEK), a slightly lower one – by those with a vinylester matrix, and a value considerably lower value than for the vinylester one – by the composites with an epoxy matrix.

The mechanical properties of composite's matrix influence considerably the crack resistance. The tests revealed that the more brittle is the composite matrix (low toughness), the lower becomes the crack resistance and, consequently, the absorbed energy AE.

Paper [1] presents the results of a critical investigation of energy release coefficients ( $G_{iC}$ ), with taking into account the influence of the matrix type and

**Table 2. SAE comparison for various types of matrix of selected structures (G – glass fibres, C – carbon fibres, A – aramid fibres), under axial loading.**

Specimen shape	Structure	Epoxy composite SAE [kJ]	Vinylester composite SAE [kJ]	PEEK resin composite SAE [kJ]	
Thin parallelepiped	Glass mat (G)	40.8	35.3	58.5	
	[(0/90) <sub>T</sub> ] <sub>S</sub> (G)	41.3	69.8	71.2	
	[(±45) <sub>T</sub> ] (G)	47.8	62.1	76.4	
	[0] <sub>9</sub> (S)	38.8	42.8	69.3	
	[0/90 <sub>T</sub> /(±45) <sub>T</sub> /0] <sub>S</sub> (G)	36.8	51.7	62.1	
	[(0/90) <sub>S</sub> ] (C)	67.7	70.3	92.5	
	[(±45) <sub>T</sub> ] (C)	65.1	68.9	89.3	
	[0] <sub>9</sub> (C)	62.4	64.9	86.9	
	[0/90 <sub>T</sub> /(±45) <sub>T</sub> /0] <sub>S</sub> (C)	60.8	62.9	81.8	
	[(0/90) <sub>S</sub> ] (A)	48.1	59.2	62.8	
	[(±45) <sub>T</sub> ] (A)	47.9	60.7	65.2	
	[0/90 <sub>T</sub> /(±45) <sub>T</sub> /0] <sub>S</sub> (A)	47.4	58.3	63.4	
Tubes	[0 <sub>3</sub> ] (G)	41.9	42.8	76.2	
	[±15/0 <sub>2</sub> ] <sub>S</sub> (G)	47.5	49.3	80.3	
	[±30/0 <sub>2</sub> ] <sub>S</sub> (G)	32.6	36.6	79.8	
	[±45/0 <sub>2</sub> ] <sub>S</sub> (G)	53.4	57.9	86.4	
	[90/0 <sub>2</sub> ] <sub>S</sub> (G)	48.6	68.9	82.5	
	[(0/90) <sub>T</sub> /0 <sub>2</sub> ] <sub>S</sub> (G)	64.2	72.9	87.1	
	[±15/0 <sub>2</sub> ] <sub>S</sub> (C)	71.3	73.3	94.9	
	[±30/0 <sub>2</sub> ] <sub>S</sub> (C)	62.1	64.7	84.8	
	[90/0 <sub>2</sub> ] <sub>S</sub> (C)	75.1	76.1	96.1	
	[(0/90) <sub>T</sub> /0 <sub>2</sub> ] <sub>S</sub> (C)	77.2	80.2	98.2	
Truncated cone $\phi =$	5°	(0/90) <sub>T</sub> /0/(0/90) <sub>T</sub> (G)	61.1	63.1	–
	10°		59.6	62.5	–
	15°		48.9	52.7	–
	20°		35.8	38.9	–
	5°	[(0/90) <sub>T</sub> ] <sub>2</sub> /0 <sub>2</sub> /[(0/90) <sub>T</sub> ] <sub>2</sub> (G)	70.2	74.2	–
	10°		69.8	71.3	–
	15°		67.8	69.9	–
	20°		61.6	64.2	–
	5°	(0/90) <sub>T</sub> /0/(0/90) <sub>T</sub> (C)	69.9	72.3	–
	10°		67.3	70.6	–
	15°		55.8	60.2	–
	20°		43.1	52.9	–
	5°	[(0/90) <sub>T</sub> ] <sub>2</sub> /0 <sub>2</sub> /[(0/90) <sub>T</sub> ] <sub>2</sub> (C)	77.3	80.2	–
	10°		76.8	78.5	–
	15°		75.4	75.9	–
	20°		68.9	71.8	–

**Table 3. SAE comparison for various types of epoxy composite reinforcements for selected structures.**

Specimen shape		Structure	Carbon roving	Carbon fabric	Glass roving	Glass fabric	aramid fabric
Plane		[0 <sub>8</sub> ]	62.4	–	40.2	–	–
		[(±45) <sub>T</sub> ]	-	65.1	-	47.8	47.9
		[(0/90) <sub>T</sub> ] <sub>10</sub>	-	67.7	-	41.3	48.1
		[0/90 <sub>T</sub> /(±45) <sub>T</sub> /0] <sub>S</sub>	–	60.8	–	36.8	47.4
Tubes		[0 <sub>8</sub> ]	62.4	–	41.9	–	–
		[±15/0 <sub>2</sub> ] <sub>S</sub>	71.3	–	47.5	–	–
		[±30/0 <sub>2</sub> ] <sub>S</sub>	62.1	–	32.6	–	–
		[±45/0 <sub>2</sub> ] <sub>S</sub>	56.8	–	53.4	–	–
		[90/0 <sub>2</sub> ] <sub>S</sub>	75.1	–	48.6	–	–
		[(0/90) <sub>T</sub> /0 <sub>2</sub> ] <sub>S</sub>	–	87.4	–	64.2	57.5
Truncated cone $\phi =$	5°	(0/90) <sub>T</sub> /0/(0/90) <sub>T</sub>	–	73.4	–	70.2	–
	10°		–	76.8	–	69.8	–
	15°		–	75.4	–	67.8	–
	20°		–	68.9	–	61.6	–
	5°	[(0/90) <sub>T</sub> ] <sub>2</sub> /0 <sub>2</sub> /[(0/90) <sub>T</sub> ] <sub>2</sub>	–	69.9	–	61.1	–
	10°		–	67.3	–	59.6	–
	15°		–	55.8	–	48.9	–
	20°		–	43.1	–	35.8	–

the load application manner (I, II, (I+II)) on the crack propagation effect (delamination) for static loads. Two types of composites were taken in the tests: an epoxy composite reinforced with unidirectional carbon fibres and one with a thermoplastic shield (PEEK) reinforced in the same way. The results of crack toughness tests for the investigated composites are presented in Table 4, where  $G_{IC}$  denotes the critical energy release coefficient. In tests, for different load cases (I, II, (I+II)) – (I – crack divergence, II – transversal shear, I+II – mixed load), the specimens DCB, ENF, CLS were assumed correspondingly – cf. paper [2].

**Table 4. Matrix type influence on  $G_{IC}$  for the carbon fibre-reinforced composites.**

Composite type	$G_{IC}$ [J/m <sup>2</sup> ]	$G_{(I-II)C}$ [J/m <sup>2</sup> ]	$G_{IIC}$ [J/m <sup>2</sup> ]
Composite C/E	473	599	650
Composite C/PEEK	1205	1397	1502

From among all the analysed composites, the one with a thermoplastic matrix PEEK, reinforced with carbon fibres, proved to be the most resistant to cracking.

It can be concluded from the results presented in Table 3 that the carbon fibres composites reveal the highest impact energy-absorbing capability, whereas the aramid fibres-reinforced ones exhibit the lowest ability. This phenomenon can be explained by the mechanical properties of the fibres. The carbon fibres have high compression and shear strength and during failure the composites undergo shear and bending of the layers. However, the aramid fibres have a very low compression strength ( $R^-$ ) but a very high tensile one ( $R^+ = 1300$  MPa), which is shown in Fig. 3.

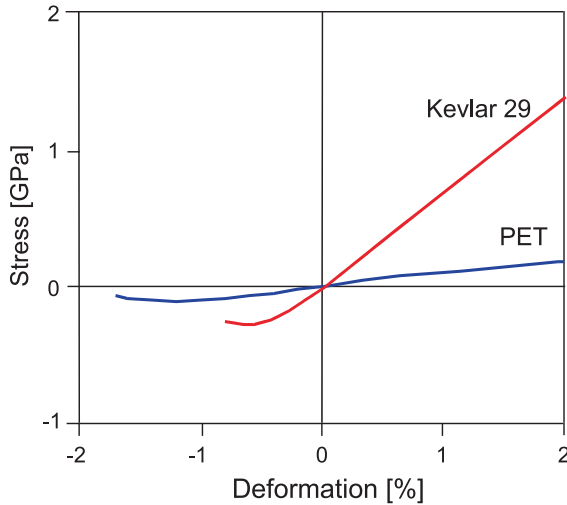


FIG. 3. The  $\varepsilon$ - $\sigma$  diagram for Kewlar 29 and polyethylene terephthalate fibres [3].

The behaviour of the epoxy composite reinforced with aramid fibres in an axial compression test was dominated by the brittle matrix and plastic fibres, which resulted in a fast progress of delamination, with plastic deformations of the fibres' layer during the failure. The mechanical properties and, in particular, the bending stiffness of the layer with aramid fibres, are lower than those for the layers reinforced with carbon and glass fibres – the AE in the case of the aramid composite was lower.

## 5. INFLUENCE OF THE COMPOSITE'S STRUCTURE

On the grounds of our own investigation, the influence of the composite's structure on the SAE was elaborated. The obtained results are shown in Figs. 4–8.

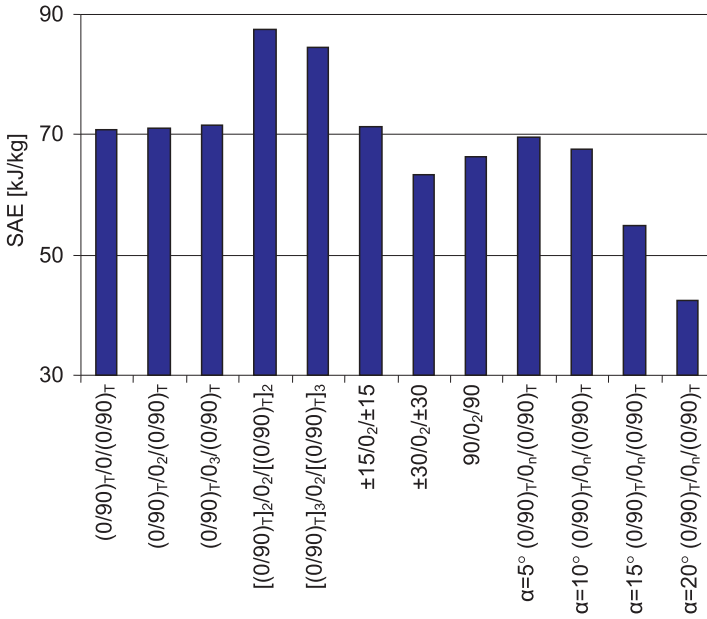


FIG. 4. Dependence of the energy-absorbing capability on the carbon-epoxy composite structure.

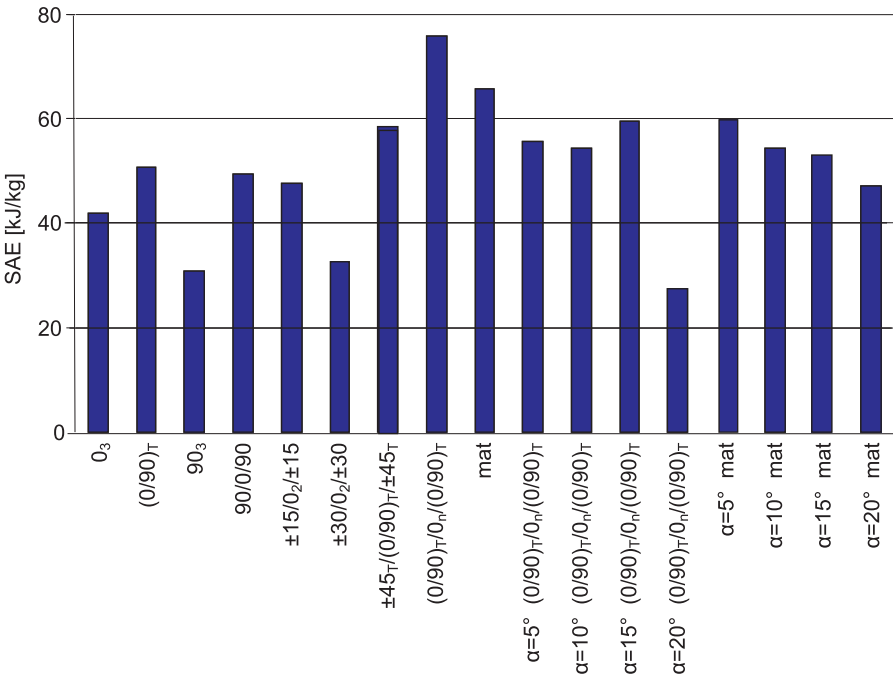


FIG. 5. Dependence of the energy-absorbing capability on the glass-epoxy composite structure.

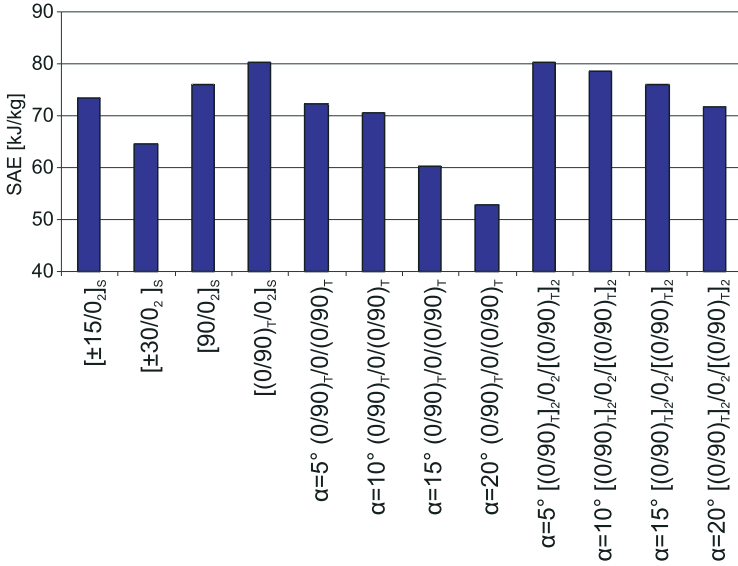


FIG. 6. Dependence of the energy-absorbing capability on the carbon-vinylester composite structure.

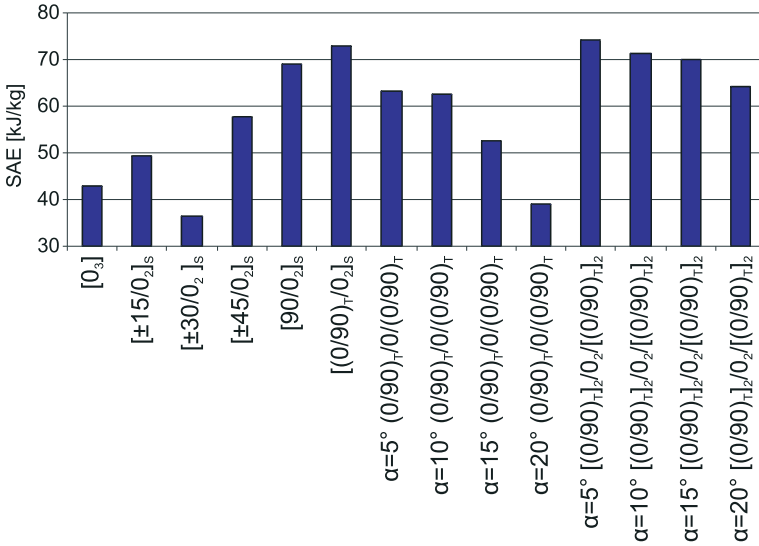


FIG. 7. Dependence of the energy-absorbing capability on the glass-vinylester composite structure.

The fibre orientation in a layer exerts the same influence on the SAE as on the mechanical properties, i.e. bending stiffness, failure deformations at tension and compression as well as on strength. The influence of the fibre orientation in a layer on the properties of the investigated composite and the composite

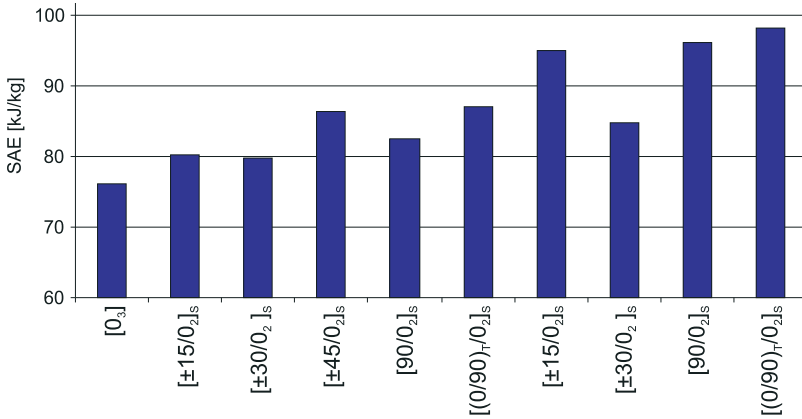


FIG. 8. Dependence of the energy-absorbing capability on the glass-PEEK composite structure.

response to the bending load during the test is clearly demonstrated in the case of a specimen reinforced with carbon fibres. The test results for the C/E  $[+45_k/-45_k]_s$  composite revealed a higher crush failure force than for the composites of the structure  $[0]_n$  and  $[90]_n$ , in spite of their lower stiffness. The C/E specimens with the  $[+45_k/-45_k]_s$  structure exhibit a larger plastic range in the test, which makes an important difference in comparison to the crush process of other C/E specimens.

The highest SAE is exhibited by the elements of the  $[(0/90)_T/0_n/(0/90)_T]$  structure, made of a carbon fibre-reinforced composite, in which the external and internal layers are made of cross-linked rowing fibres, which carry on the circumferential stresses, whereas the external layers consist of rowing parallel to the specimen's axis, which causes an increased compressive and bending strength.

## 6. INFLUENCE OF THE WALL THICKNESS OF ENERGY-ABSORBING STRUCTURE ELEMENTS

The basis for elaborating the SAE dependence on the element wall's thickness were the results of our own test, presented in Fig. 9, in which these relations are to a great extent approximated by straight lines. Very thin elements fail by local buckling, which is caused by low value of the SAE. The relation SAE-thickness of an energy-absorbing element can serve in practice to design an energy-absorption structure of a vehicle or an aircraft with a requested value of AE.

With a given kinetic energy of the crash, one can calculate the required absorption energy and next, while selecting the sandwich structure, assume the appropriate wall thickness of an element used as a core in the shape of a tube, a truncated cone, a sphere or a waved shell.

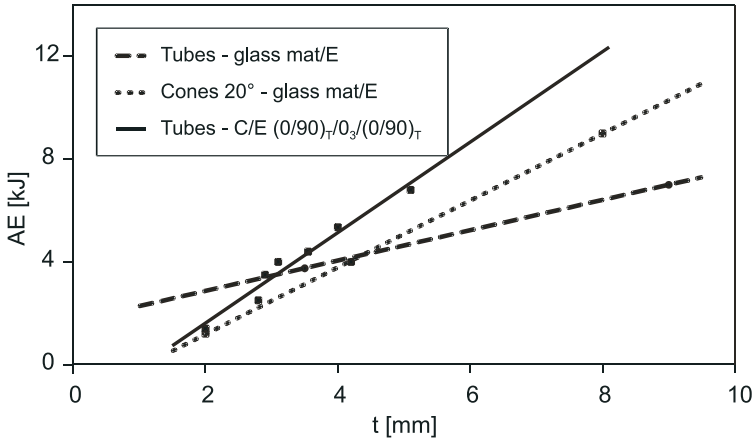


FIG. 9. Dependence of AE on the element wall's thickness.

The dependence of the AE on the element's thickness is very significant and clearly visible in the energy absorption tests. The composite's thickness influences the bending stiffness and failure of composite elements, which is clearly visible from the slope of the force-displacement curve in the first stage. A larger thickness results in a larger moment of inertia and a larger bending stiffness ( $EI$ ), which in turn causes an increase of the bending resistance of the element and in the force necessary to reach the required failure deformation. Along with the increase of thickness, the composite layers become more stiff and they require higher deformation and failure forces.

The bending stiffness ( $EI$ ), and in particular the specimen's thickness, affects the composite's AE, because the moment of inertia of the cross-section depends on the third power of the stiffness ( $I = wt^3/12$ ). The bending stiffness depends, of course, on the Young's modulus  $E$ , which in turn depends on the type and structure of the composite.

## 7. INFLUENCE OF THE LAYER'S THICKNESS IN THE COMPOSITE ON THE SAE

In order to study the influence of the layers' thickness in the composite on the SAE value, the results of tests shown in Tables 5 and 6 were used. The dependence of the SAE on the ratio of the middle layer wall thickness  $t_m$  of the composite in respect to the external one ( $t_m/t_e$ ), for carbon-epoxy and glass-epoxy composites is given in Fig. 11. From this relation it follows that for the glass-epoxy composite the maximum value of SAE occurs at  $t_m/t_e \approx 3.0$ . However, in the case of the carbon-epoxy composite the SAE is independent of the layer ratio ( $t_m/t_e$ ).

Table 5. Properties of specimens made of carbon-epoxy composite.

Specimen number	Structure	$\alpha$ [°]	$t$ [mm]	$D_i$ [mm]	$t_i$ [mm]	$t_m$ [mm]	$t_e$ [mm]	$h$ [mm]	$z$ [%]	$m$ [g]	$P_{\max}$ [kN]	$P_{\text{avg}}$ [kN]	AE [J]	SAE [kJ/kg]
1-4	(0/90) <sub>T</sub> /0/(0/90) <sub>T</sub>	5	1.2	59.5	0.4	0.4	0.4	75.0	42	22.8	24.4	21.4	1602	70.3
2-4	(0/90) <sub>T</sub> /0 <sub>2</sub> /(0/90) <sub>T</sub>	5	2.0	59.4	0.5	1.0	0.5	85.6	42	39.5	39.5	32.3	2761	69.9
3-4	(0/90) <sub>T</sub> /0 <sub>3</sub> /(0/90) <sub>T</sub>	5	2.2	59.5	0.4	1.4	0.4	83.4	42	42.2	46.2	34.7	2896	68.6
6-4	(0/90) <sub>T</sub> /0/(0/90) <sub>T</sub>	10	1.2	59.4	0.4	0.4	0.4	78.8	42	21.5	21.5	17.0	1336	62.2
7-4	(0/90) <sub>T</sub> /0 <sub>2</sub> /(0/90) <sub>T</sub>	10	2.4	59.7	0.6	1.2	0.6	83.6	42	41.3	44.8	35.1	2924	70.8
8-4	(0/90) <sub>T</sub> /0 <sub>3</sub> /(0/90) <sub>T</sub>	10	3.2	59.8	0.6	2.0	0.6	84.9	42	71.0	72.8	58.4	4924	69.4
11-4	(0/90) <sub>T</sub> /0/(0/90) <sub>T</sub>	15	1.2	58.8	0.4	0.4	0.4	54.1	42	17.4	18.1	16.5	892	51.3
12-4	(0/90) <sub>T</sub> /0 <sub>2</sub> /(0/90) <sub>T</sub>	15	2.0	59.2	0.5	1.0	0.5	58.0	42	23.7	27.3	22.8	1322	55.8
13-4	(0/90) <sub>T</sub> /0 <sub>3</sub> /(0/90) <sub>T</sub>	15	3.2	58.9	0.6	2.0	0.6	62.4	42	42.0	52.5	38.9	2426	57.8
16-4	(0/90) <sub>T</sub> /0/(0/90) <sub>T</sub>	20	1.2	79.5	0.4	0.4	0.4	67.0	42	25.2	14.7	13.6	911	36.4
17-4	(0/90) <sub>T</sub> /0 <sub>2</sub> /(0/90) <sub>T</sub>	20	2.0	78.8	0.5	1.0	0.5	68.9	42	36.0	27.9	22.5	1552	43.1
18-4	(0/90) <sub>T</sub> /0 <sub>3</sub> /(0/90) <sub>T</sub>	20	2.5	79.5	0.5	1.5	0.5	68.4	42	49.9	40.0	34.7	2373	47.6
21-4	(0/90) <sub>T</sub> /0/(0/90) <sub>T</sub>	0	1.7	39.3	0.6	0.5	0.6	98.2	42	28.5	21.1	27.7	2075	70.9
24-4	(0/90) <sub>T</sub> /0 <sub>2</sub> /(0/90) <sub>T</sub>	0	2.3	39.3	0.6	1.1	0.6	98.0	42	35.6	25.4	32.2	2489	71.0
28-4	(0/90) <sub>T</sub> /0 <sub>3</sub> /(0/90) <sub>T</sub>	0	3.0	39.3	0.6	1.8	0.6	102.2	42	54.6	39.4	54.5	4027	71.6
2-5	[(0/90) <sub>T</sub> ] <sub>2</sub> /0 <sub>2</sub> /[(0/90) <sub>T</sub> ] <sub>2</sub>	0	3.0	39.3	1.0	1.0	1.0	80.2	41	41.6	65.1	49.0	2586	87.4
5-5	[(0/90) <sub>T</sub> ] <sub>2</sub> /0 <sub>2</sub> /[(0/90) <sub>T</sub> ] <sub>2</sub>	5	2.1	59.5	0.7	0.7	0.7	76.3	41	35.7	43.9	35.67	2722	76.2
6-5	[(0/90) <sub>T</sub> ] <sub>2</sub> /0 <sub>2</sub> /[(0/90) <sub>T</sub> ] <sub>2</sub>	10	2.1	59.8	0.7	0.7	0.7	77.3	41	36.4	45.8	37.25	2879	79.1
7-5	[(0/90) <sub>T</sub> ] <sub>2</sub> /0 <sub>2</sub> /[(0/90) <sub>T</sub> ] <sub>2</sub>	15	2.1	59.3	0.7	0.7	0.7	50.6	41	24	64.2	36.16	1830	76.2
8-5	[(0/90) <sub>T</sub> ] <sub>2</sub> /0 <sub>2</sub> /[(0/90) <sub>T</sub> ] <sub>2</sub>	20	2.4	79.4	0.8	0.8	0.8	66.1	41	50.4	68.3	48.58	3211	63.7
9-5	[(0/90) <sub>T</sub> ] <sub>3</sub> /0 <sub>2</sub> /[(0/90) <sub>T</sub> ] <sub>3</sub>	0	3.6	39.3	1.4	0.8	1.4	81.2	42	50.1	67.5	52.34	4250	84.5
11-5	[(0/90) <sub>T</sub> ] <sub>3</sub> /0 <sub>2</sub> /[(0/90) <sub>T</sub> ] <sub>3</sub>	5	2.9	59.2	1.1	0.7	1.1	83.5	42	49.4	57.8	45.92	3834	77.6
12-5	[(0/90) <sub>T</sub> ] <sub>3</sub> /0 <sub>2</sub> /[(0/90) <sub>T</sub> ] <sub>3</sub>	10	2.9	60.1	1.1	0.7	1.1	82.8	42	53.5	57.7	49.43	4093	76.5
13-5	[(0/90) <sub>T</sub> ] <sub>3</sub> /0 <sub>2</sub> /[(0/90) <sub>T</sub> ] <sub>3</sub>	15	3.2	59.3	1.2	0.8	1.2	58.7	42	44.5	72.1	56.41	3311	74.4
14-5	[(0/90) <sub>T</sub> ] <sub>3</sub> /0 <sub>2</sub> /[(0/90) <sub>T</sub> ] <sub>3</sub>	20	4.2	79.5	1.6	1.0	1.6	68.4	42	81.3	116	83.34	5700	70.1
16-5	$\pm 15/0_2/\pm 15$	0	4.1	39.3	1.4	1.3	1.4	80.5	57	67.9	73.1	60.16	4843	71.3
18-5	$\pm 30/0_2/\pm 30$	0	3.8	39.3	1.3	1.2	1.3	81.2	59	56.1	58	42.92	3485	62.1
21-5	90 <sub>2</sub> /0 <sub>2</sub> /90 <sub>2</sub>	0	4.1	39.3	1.4	1.3	1.4	81.2	56	63.5	67	52.63	4274	67.3

Table 6. Properties of specimens made of glass-epoxy composite.

Specimen number	Structure	$\alpha$ [°]	$t$ [mm]	$D_i$ [mm]	$t_i$ [mm]	$t_m$ [mm]	$t_e$ [mm]	$h$ [mm]	$z$ [%]	$m$ [g]	$P_{\max}$ [kN]	$P_{\text{avg}}$ [kN]	AE [J]	SAE [kJ/kg]
1-1	mat	0	3.5	39.3	-	-	-	86.7	35	59.4	52.6	43.8	3788	63.7
4-1	mat	0	9	39.3	-	-	-	91	35	168.3	137.4	117.7	10706	63.6
7-1	mat	5	2	60	-	-	-	91.2	35	35.9	20.7	16.6	1511	42.1
8-1	mat	5	2.7	61.6	-	-	-	93.2	35	65.7	47	39.2	3646	55.5
9-1	mat	5	4	61	-	-	-	91.1	35	100.1	70.2	59.5	5415	54.2
10-1	mat	5	5.2	59.6	-	-	-	92	35	123.4	88.4	75.6	6955	56.4
11-1	mat	10	1.5	61	-	-	-	82.3	35	31.7	18.9	15.6	1279	40.4
12-1	mat	10	1.8	62.4	-	-	-	85.2	35	36.5	26.1	20.2	1717	47.0
13-1	mat	10	2.3	60.4	-	-	-	86.3	35	46	34.3	24.9	2141	46.6
14-1	mat	10	3.2	60.6	-	-	-	91.9	35	68.4	54.7	42.1	3831	56.0
15-1	mat	10	4.2	60.6	-	-	-	91.7	35	81.4	72.6	56	5096	62.6
16-1	mat	10	5.5	61	-	-	-	84.3	35	111.4	99.7	80.8	6787	60.9
18-1	mat	15	3.4	59.2	-	-	-	62.6	35	48.4	56.9	41.8	2592	53.5
19-1	mat	15	4.2	59.6	-	-	-	62.3	35	59.9	69.1	54.7	3391	56.6
20-1	mat	15	5	60	-	-	-	62.5	35	73.9	88.3	67.6	4191	56.7
21-1	mat	15	6.4	60.2	-	-	-	62.4	35	99.2	132.3	98.5	6107	61.6
22-1	mat	20	2	80	-	-	-	70.8	35	45.5	27.5	18.6	1302	28.6
23-1	mat	20	4.2	80.6	-	-	-	70.2	35	92.4	77.5	59.2	4144	44.8
24-1	mat	20	8	79	-	-	-	64.2	35	162.3	175.5	143.5	9184	56.6
1-2	90/0 <sub>2</sub> /90	0	2.4	39.3	0.6	1.2	0.6	80.9	55	37.5	21.9	18.6	1597	42.6
4-2	(±45 <sub>T</sub> ) <sub>2</sub> /0 <sub>2</sub> /((±45 <sub>T</sub> ) <sub>2</sub> )	0	3.4	39.3	1.1	1.2	1.1	90.1	49	53.4	34.1	31.7	2853	53.4
7-2	[±45 <sub>T</sub> ] <sub>2</sub>	0	1.4	39.3	-	-	-	59.9	45	20.0	13.8	11.0	659	32.9
11-2	[(0/90) <sub>T</sub> ] <sub>2</sub>	0	1.4	39.3	-	-	-	60.1	46	19.9	15.9	13.2	791	40.1
1-3	90/0/90	0	2	39.3	0.7	0.6	0.7	96	58	43.4	34.5	20.3	1953	45.0
4-3	90 <sub>2</sub> /0 <sub>2</sub> /90 <sub>2</sub>	0	3.7	39.3	1.2	1.3	1.2	89.8	56	84.8	62.5	51.0	4582	54.0
7-3	90 <sub>3</sub> /0 <sub>3</sub> /90 <sub>3</sub>	0	5.2	39.3	1.7	1.8	1.7	94.4	56	128.3	75.6	66.3	6260	48.8
10-3	[(0/90) <sub>T</sub> ] <sub>2</sub> /0 <sub>2</sub> /((0/90) <sub>T</sub> ) <sub>2</sub>	0	4.5	39.3	1.5	1.5	1.5	94.7	49	79.8	66.8	62.7	5921	74.1
13-3	[(0/90) <sub>T</sub> ] <sub>4</sub> /0 <sub>4</sub> /((0/90) <sub>T</sub> ) <sub>4</sub>	0	7	39.3	2.3	2.4	2.3	97.3	48	150.7	164.2	120.0	11680	77.4
16-3	(±45 <sub>T</sub> ) <sub>2</sub> /[(0/90) <sub>T</sub> ] <sub>2</sub> /((±45 <sub>T</sub> ) <sub>2</sub> )	0	4.5	39.3	1.5	1.5	1.5	92.6	44	84.1	69.0	53.0	4895	58.4
19-3	±15/0 <sub>2</sub> /±15	0	4.5	39.3	1.5	1.5	1.5	99.1	55	97.3	50.2	41.0	4070	47.5
22-3	0 <sub>3</sub>	0	2.5	39.3	-	-	-	96.6	54	50.7	32.1	22.0	2126	41.9
25-3	90 <sub>3</sub>	0	3	39.3	-	-	-	80.7	55	60.3	32.8	23.0	1856	30.8
27-3	±30/0 <sub>2</sub> /±30	0	4.4	39.3	1.5	1.4	1.5	93.6	56	94.7	43.3	33.0	3085	32.6

The obtained different relations for glass-epoxy and carbon-epoxy composites result from the difference in adhesion of fibres to the epoxy resin, which in the case of carbon fibres is larger than for the glass fibres. Moreover, the shear resistance in the planes parallel to the fibres, for composites of the  $[0^\circ]_n$  structure, for the carbon-epoxy composite is 20.6 MPa and for the glass epoxy one – only 8.8 MPa, which means that for the carbon-epoxy composites it is 2.3 times higher. For  $t_m/t_e = \infty$ , i.e. for the carbon-epoxy composite of the  $[0^\circ]_n$  structure, the SAE value is 76.2 kJ, which is approximately equal to the averaged SAE value for  $t_m/t_e = (1 - 5)$ .

The results of testing, averaged from several tests and included in Tables 5 and 6, are determined by characteristic quantities, denoting as follows (see Fig. 10):

$P_{\max}$  – maximum crush failure force, i.e. the first peak on the  $P - \Delta l$  curve, which demonstrates the failure initiation;

AE – absorbed energy, equivalent to the area under the  $P - \Delta l$  curve;

$P_{\text{avg}}$  – average crush failure force ( $P_{\text{avg}} = \text{AE}/\Delta l_{\text{max}}$ );

SAE – specific absorbed energy  $\text{SAE} = \text{AE}/m_c$ , where  $m_c$  is the mass of the destroyed part of the specimen;

$\alpha$  – cone vertex half-angle;

$t$  – wall thickness;

$D_i$  – internal diameter (for a cone – the major diameter or the base diameter);

$t_i$  – thickness of the internal layer;

$t_m$  – thickness of the middle layer;

$t_e$  – thickness of the external layer;

$h$  – height of the specimen;

$z$  – weight content of fibres in the composite;

$m$  – mass of the specimen;

$\gamma$  – force uniformity index ( $P_{\text{avg}}/P_{\text{max}}$ ).

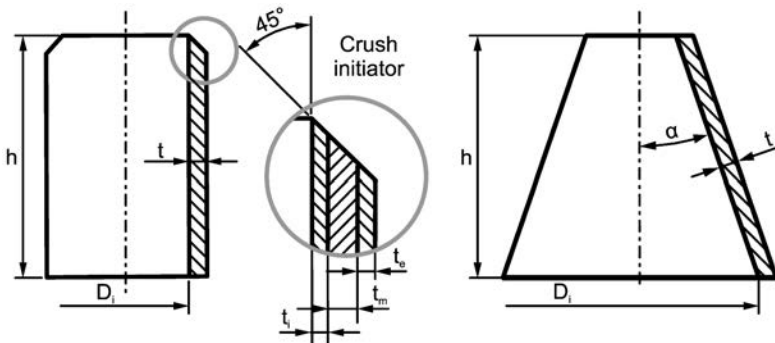


FIG. 10. Shapes of specimens used in tests.

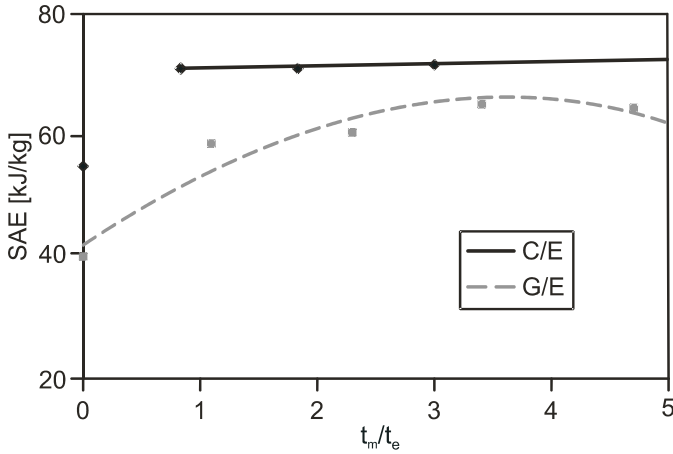


FIG. 11. Influence of the composite layers' thickness on the SAE.

#### 8. INFLUENCE OF THE ENERGY-ABSORBING STRUCTURES' ELEMENTS ON THE SAE (FOR SELECTED STRUCTURES)

It follows from the data presented in Table 7 that the highest SAE value is exhibited by the energy absorbing elements in the shape of a tube with a ring cross-section; next come truncated cones, plane shells and waved shells; the lowest SAE is revealed by spheres. The lowest value of SAE for the element in the shape of a sphere is caused by its specific failure mode. During failure, neither brittle fragmentation of the element's wall occurs nor the fibres' cracking takes place. Instead, the sphere's wall is bent into inside with permanent deformation, which is presented in Fig. 12.



FIG. 12. Cross-section of the destroyed sphere shows delamination of the plays.

It should be underlined that the influence of the shape of an energy-absorbing structure element is important not only from the point of view of the SAE value, but also because of the dependence of the acceleration during impact. In order

**Table 7. Comparison of SAE for different shapes of the energy-absorbing elements.**

Composite type	Structure	Plane element	Tube	Truncated cone	Waved shell	Spherical shell
G/E	mat	40.8	63.5	55.3 (5°) 44.8 (20°)	38.9	11.8
G/E	[(0/90) <sub>T</sub> ] <sub>S</sub>	41.3	44.2	51.1 (5°) 35.8 (20°)	39.5	24.3
G/E	[(±45) <sub>T</sub> ] <sub>n</sub>	47.8	53.4	56.5 (5°) 38.3 (20°)	30	
G/E	[(0/90) <sub>T</sub> /0 <sub>2</sub> ] <sub>S</sub>	44.1	64.2	61.2 (5°) 36.8 (20°)		
C/E	[0] <sub>n</sub>	62.4	72.8	–	–	–
C/E	[±15/0 <sub>2</sub> ] <sub>S</sub>	62.0	71.3	–	–	–
C/E	[±30/0 <sub>2</sub> ] <sub>S</sub>	58.0	62.1	–	–	–
C/E	[±45/0 <sub>2</sub> ] <sub>S</sub>	65.1	58.4	–	–	–
C/E	[(0/90) <sub>T</sub> /0] <sub>S</sub>	67.7	75.1	69.9 (5°) 43.1 (20°)	72.1	–
A/E	[±45/0 <sub>2</sub> ] <sub>S</sub>	62.0	57.9	–	–	–
A/E	[(0/90) <sub>T</sub> /0] <sub>S</sub>	52.6	68.9	–	–	13.6
G/VE	[0] <sub>n</sub>	42.8	42.8	–	–	–
G/VE	[(±45) <sub>T</sub> ]	52.1	57.9	–	–	–
G/VE	[(0/90) <sub>T</sub> /0] <sub>S</sub>	49.8	72.9	63.1 (5°) 38.9 (20°)	–	–
C/VE	[0] <sub>n</sub>	69.6	64.9	–	–	–
C/VE	[(0/90) <sub>T</sub> ] <sub>n</sub>	70.7	75.7	–	–	–
C/VE	[±45] <sub>n</sub>	56.8	64.7	–	–	–
G/PEEK	mat	58.5	76.2	–	–	–
G/PEEK	[(0/90) <sub>T</sub> ] <sub>n</sub>	71.2	82.5			

to determine the influence of the specimen's shape on the acceleration course at impact, we shall analyse the  $P - \Delta l$  dependence obtained from tests for tubes, truncated cones, waved shells and spheres – Fig. 13.

On the grounds of the above results for the  $P - \Delta l$  dependence, for specimens of the same thickness we conclude that the largest change of the crush failure force during loading and – consequently – a large SAE is exhibited by the energy-absorbing elements in the shape of tubes and corrugated shells, whereas a lower SAE was revealed by truncated cones and the lowest one – by spheres. Analogically to the load change, the maximum peaks of acceleration will occur during impact.

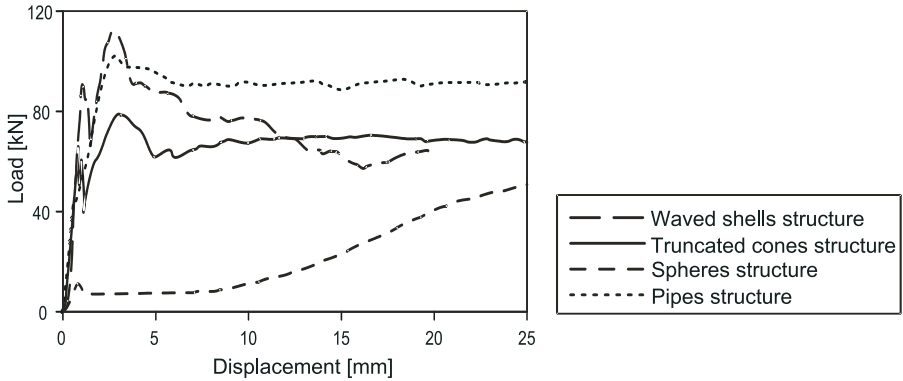


FIG. 13.  $P - \Delta l$  dependence for a tube, a truncated cone, a waved shell and a sphere made of epoxy composite reinforced with a glass mat.

## 9. SUMMARY

1. Exhaustive results of investigation presented in this paper and preliminary calculations included in its first part enable us to design an energy-absorbing structure with a programmed value of absorption energy of a given equipment under axial loading.
2. From all the analysed materials for energy-absorbing structures, the polymer composites are the most expensive, which was shown in Table 1, but a relatively cheap epoxy composite reinforced with a glass mat revealed in testing a relatively high AE with respect to its density.
3. The influence of the matrix type (resin) in a composite on the SAE is considerable. A large part in the ability of energy absorption is due to the mechanical properties of the matrices, in particular – their crack resistance. Brittle matrices, such as epoxy ones, reveal a lower ability of energy absorption, whereas the composites with a polyetherketone matrix proved to have the highest SAE.
4. The influence of the reinforcement type on the SAE is the following: carbon fibres have the highest SAE, whereas the aramid ones – the lowest. The carbon fibres have highest compressive and shearing strength, whereas for the aramid ones both strengths are low.
5. On the basis of various structures testing, one can conclude that the energy-absorbing structure should contain stiff and resistant middle layers, whereas the external ones should carry well the transversal stresses (circumferential in the case of a pipe). The influence of fibres orientation in an energy-absorbing element is the same on the bending and shear strength. The highest SAE was obtained for the  $[(0/90)_T/0_n/(0/90)_T]$  structure with

the external layers made of fabric and the internal one – of continuous fibres aligned parallel to the compressive force.

6. The influence of the wall thickness of an energy-absorbing element on the SAE was presented in Fig. 7. Along with the increase of wall's thickness, the SAE increases because the bending strength of the wall grows also and it is the layers' bending that prevails in the failure process. Also, the influence of the layers' thickness in the composite on the SAE was considered. It was found that the ratio of the middle layer thickness to that of the external layers for the carbon fibre-reinforced composite is small.

#### REFERENCES

1. S. MALL, K. T. YUN, N. K. KOCHHAR, *Characterization of matrix toughness effect on cyclic delamination growth in graphite fiber composites*, Composite Materials, Fatigue and Fracture, **2**, 1989.
2. S. OCHELSKI, *Experimental methods in the mechanics of structural composites* [in Polish], WNT, Warsaw 2004.
3. S. KAWABATA, Y. YAMASHITA, M. NIWA, *Micro-mechanics of wool single fibre*, 10th International Wool Textile Research Conference, Aachen, Germany 2000.

*Received June 2, 2008; revised version October 22, 2008.*

---